HEAT AND MOISTURE TRANSFER THROUGH POROUS ROOF

Gerson Henrique dos Santos, ghsantos@ufpr.br
Universidade Federal do Paraná (UFPR)
Department of Mechanical Engineering - 81531-990 - Curitiba, Brazil

Nathan Mendes, nathan.mendes@pucpr.br
Pontifícia Universidade Católica do Paraná (PUCPR)
Department of Mechanical Engineering - 80.215-901-Curitiba, Brazil

Abstract. *Since the 70's, the environmental concerns and the rational use of the available energy are of paramount importance. In this context, the construction sector is widely involved in this subject, since residential, commercial and public buildings are worldwide responsible for great part of the electricity consumption. Aiming to increase building energy efficiency, some computer simulation tools have been developed. However, simplifications on the building envelope model may provide unrealistic results. Combined analysis of heat and moisture transport through porous building elements is barely explored in the literature due to many difficulties such as modeling complexity, computer run time, numerical convergence and highly moisture-dependent properties. In this context, a mathematical model to simulate an unsaturated highly capacitive porous roof is considered for studying its effects on building passive cooling. The TRY (Test Reference Year) weather data of Curitiba, Brazil, was utilized for external boundary conditions and comparisons in terms of temperature and relative humidity at the roof surfaces are presented.*

Keywords*: porous media, building simulation, passive cooling.*

1. INTRODUCTION

Since the seventies, due to the worldwide energy crisis, some countries have adopted a severe legislation aiming to promote energy efficiency of equipment and buildings and to evaluate the building performance with thermal parameters, several codes have been developed. However, most of those codes do not take into account the moisture presence within building envelopes. The moisture in the envelope of buildings implies an additional mechanism of transport absorbing or releasing latent heat of vaporization, affecting the hygrothermal building performance or causing mold growth (Santos and Mendes, 2009a, 2009b, 2009c).

In this context, a layer of humid porous medium, such as humid sand layer on the roof can counterbalance the heating of fervent solar radiation and outdoor air temperature, which can produce passive cooling effect, mainly for low-rise buildings with large roof area (Meng and Hu, 2005). In other work, LIU et. al. (1995) showed that the free evaporative cooling in or on an unsaturated porous packed bed that works as a part of roofs or walls in buildings is a highly promising project due to its engineering background and theoretical interests. This method of cooling may be used in designing a useful air-conditioning device that could be installed in private houses and public buildings to transfer heat flux from rooms to ambient air, thereby reducing the temperature of the room by the free evaporation effect in pore spaces and on the surface exposed directly to atmosphere.

On the other hand, combined heat and moisture transfer in porous media may require the use of very short time steps in the simulations, especially at highly permeable surfaces, which may prohibit the use of long time step for long-term simulations due to the numerical instabilities caused by the effect of latent heat at the boundaries. Combined heat and moisture transport in porous materials often occurs and is very interactive especially in building envelope components, such as roofs and exterior walls. The complex nature of these transport processes makes it difficult to develop general methods for calculations. However, calculation methods are powerful tools for building designers and practitioners to assess the thermal and hygric effects of heat and moisture transport, and to generate guidelines and practices for controlling the moisture response (Wang and Hagentoft, 2001).

The mathematical description for predicting envelope building hygrothermal dynamics is complex, due to non-linearities and interdependence among several variables. The parametric uncertainties in the modeling, simulation time steps, external climate, building schedules, hygrothermal properties and moisture storage and transport also contribute to increase this complexity. In this case, for ensuring numerical stability in the present model, the linearized set of equations was obtained by using the finite-volume method and the MultiTriDiagonal-Matrix Algorithm (Mendes et. al., 2002) to solve a 1-D model to describe the physical phenomena of heat and mass transfer in the building envelope (roof), including the sand layer. In this way, the code has been conceived to be numerically robust with a fast-simulating procedure. The heat and moisture transfer in envelope building was based on the theory of Philip and De Vries (1957), which is one of the most disseminated and accepted mathematical formulation for studying heat and moisture transfer through porous media, considering both vapor diffusion and capillary migration.

In this paper, the weather data of Curitiba-Brazil was utilized for external boundary conditions and comparisons in terms of temperature and relative humidity in the roof surfaces are presented in order to predict its effects on building passive cooling.

2. MATHEMATICAL MODEL

The governing equations, based on the theory of Philip and De Vries (1957), to model heat and mass transfer through porous media, are given by Eqs. (1) and (2). The energy conservation equation is written in the form:

$$\rho_0 c_m(T,\theta)\frac{\partial T}{\partial t} = \nabla.(\lambda\ (T,\theta)\nabla T) - L(T)(\nabla.\mathbf{j}_v) \tag{1}$$

and the mass conservation equation as

$$\frac{\partial \theta}{\partial t} = -\nabla.\left(\frac{\mathbf{j}}{\rho_l}\right), \tag{2}$$

where ρ_0 is the solid matrix density (m³/kg), c_m, the mean specific heat (J/kg K), T, temperature (°C), t, time (s), λ, thermal conductivity (W/m K), L, latent heat of vaporation (J/kg), θ, volumetric moisture content (m³/m³), j_v, vapor flow (kg/m² K), j, total flow (kg/m² K) and ρ_l the water density (kg/m³).

The total flow (j), in the 1-D model, is given by summing the vapor flow (j_v) and the liquid flow (j_l). The total moisture flow can be calculated as

$$\frac{\mathbf{j}}{\rho_l} = -\left(D_T(T,\theta)\frac{\partial T}{\partial x} + D_\theta(T,\theta)\frac{\partial \theta}{\partial x}\right)\mathbf{i}, \tag{3}$$

with $D_T = D_{Tl} + D_{Tv}$ and $D_\theta = D_{\theta l} + D_{\theta v}$, where D_{Tl} is the liquid phase transport coefficient associated to a temperature gradient (m²/s K), D_{Tv}, vapor phase transport coefficient associated to a temperature gradient (m²/s K), $D_{\theta l}$, liquid phase transport coefficient associated to a moisture content gradient (m²/s), $D_{\theta v}$, vapor phase transport coefficient associated to a moisture content gradient (m²/s), D_T, mass transport coefficient associated to a temperature gradient (m²/s K) and D_θ, mass transport coefficient associated to a moisture content gradient (m²/s). In this case, siphon potential in porous media is much bigger than gravity potential, and therefore, the latter is neglected;

The model presented for predicting heat and moisture transfer through porous roof does not take into account convection and radiation heat transfer in the pores. In the mass balance, the water vapor - classified as a perfect gas due to the low vapor partial pressure - is considered to have a much lower mass than the liquid phase.

2.1 Boundary Conditions

The upper surface of the roof is exposed to short wave radiations, convection heat transfer and phase change as boundary conditions.

In this way, at *external surface*, the energy balance becomes

$$\left(\lambda(T,\theta)\frac{\partial T}{\partial y}\right)_{y=H} + \left(L(T)j_v\right)_{y=H} = h\left(T_\infty - T_{y=H}\right) + \alpha q_r + L(T)h_m\left(\rho_{v,\infty} - \rho_{v,y=H}\right), \tag{4}$$

where $h\left(T_\infty - T_{y=H}\right)$ represents the heat exchanged by convection with the external air, described by the surface conductance h, αq_r is the absorbed short-wave radiation and $L(T)h_m\left(\rho_{v,\infty} - \rho_{v,y=H}\right)$, the phase change energy term. The loss from long-wave radiation is defined as R_{ol} (W/m²), ε, the surface emissivity. The solar absorptivity is represented by α and the mass convection coefficient by h_m, which is related to h by the Lewis' relation. In the internal surface, the radiation term was removed.

Similarly, the mass balance at the upper surface is written as

$$\left(D_\theta(T,\theta)\frac{\partial \theta}{\partial y} + D_T(T,\theta)\frac{\partial T}{\partial y}\right)_{y=H} = \frac{h_m}{\rho_l}\left(\rho_{v,\infty} - \rho_{y=H}\right). \tag{5}$$

Equations (4) and (5) show a vapor concentration difference, $\Delta\rho_v$, on their right-hand side. This difference is between the porous surface and air and is normally determined by using the values of previous iterations for temperature and moisture content, generating additional instability.

Due to numerical instability problems created by this source term, the solution of the linear set of discretized equations requires the use of very small time steps, which can be exceedingly time consuming especially in long-term

simulations. In order to rise the simulation time step, Mendes et al. (2002) presented a procedure to calculate the vapor flow, independently of previous values of temperature and moisture content. In this way, the term ($\Delta\rho_v$) was linearized as a linear combination of temperature and moisture content, viz.,

$$\left(\rho_{v,\infty} - \rho_v(s)\right) = M_1(T_\infty - T(s)) + M_2(\theta_\infty - \theta(s)) + M_3 \ , \tag{6}$$

with

$$M_1 = A\frac{M}{\Re}\phi \ ,$$

$$M_2 = \frac{M}{\Re}\left(\frac{P_s(s)}{T(s)}\right)^{prev}\left(\frac{\partial\phi}{\partial\theta(s)}\right)^{prev} ,$$

$$M_3 = \frac{M}{\Re}\left[\left(\frac{P_s(s)}{T(s)}\right)^{prev} R(\theta^{prev}(s)) + \phi_\infty(R(T_\infty) - R(T^{prev}(s)))\right],$$

where

R is a residual function of $\left(\frac{P_s}{T}\right)$, $P_{s,}$ saturated pressure (Pa), $\Re$, universal gas constant (J/kmol K), M, molecular mass (kg/kmol), ϕ , relative humidity, *prev*, previous iteration and A is the straight-line coefficient from the approximation $\left(\frac{P_s}{T}\right) = AT + B$.

2.2 Discretized Conservation Equations Solution of the Porous Element Domain

Implicit schemes demand the use of an algorithm to solve tridiagonal systems of linear equations. One of the most used is the well-known Thomas Algorithm or TDMA (TriDiagonal-Matrix Algorithm). However, for strongly-coupled equations of heat transfer problems, a more robust algorithm may be necessary in order to achieve numerical stability.

Therefore, the MTDMA (MultiTriDiagonal-Matrix Algorithm) emerged from the need of obtaining all the dependent variable profiles simultaneously at a given time step avoiding numerical divergence caused by the evaluation of coupled terms from previous iteration values.

For a physical problem represented by M dependent variables, the discretization of MxN differential equations, leads to the following system of algebraic equations,

$$\mathbf{A_i}.\mathbf{x_i} = \mathbf{B_i}.\mathbf{x_{i+1}} + \mathbf{C_i}.\mathbf{x_{i-1}} + \mathbf{E_i} \tag{7}$$

where $\mathbf{x}$ is a vector containing the M dependent variables T and θ

$$\mathbf{x}_i = \begin{bmatrix} T \\ \theta \end{bmatrix}. \tag{8}$$

Differently from the traditional TDMA, coefficients $\boldsymbol{A}$, $\boldsymbol{B}$ and $\boldsymbol{C}$ are MxN matrices, in which each line corresponds to one dependent variable. The elements that do not belong to the main diagonal are the coupled terms for each conservation equation. $\boldsymbol{E}$ is an M-element vector.

As MTDMA has the same essence as TDMA, it is necessary to replace Eq. (7) by relationships of the form

$$\mathbf{x_i} = \mathbf{P_i}.\mathbf{x_{i+1}} + \mathbf{q_i} \ , \tag{9}$$

where $\mathbf{P}_i$ is now a MxN matrix.

In the same way, vector $\mathbf{x}_{i-1}$ can be expressed in terms of $\mathbf{x}_{i+1}$,

$$\mathbf{x_{i-1}} = \mathbf{P_{i-1}}.\mathbf{x_i} + \mathbf{q_{i-1}} \ . \tag{10}$$

Substitution of Eq. (10) into Eq. (7) gives

$$\mathbf{A_i}.\mathbf{x_i} = \mathbf{B_i}.\mathbf{x_{i+1}} + \mathbf{C_i}.\left(\mathbf{P_{i-1}}.\mathbf{x_i} + \mathbf{q_{i-1}}\right) + \mathbf{E_i} \tag{11}$$

or, rearranging,

$$\left(\mathbf{A_i} - \mathbf{C_i}.\mathbf{P_{i-1}}\right).\mathbf{x_i} = \mathbf{B_i}.\mathbf{x_{i+1}} + \mathbf{C_i}.\mathbf{q_{i-1}} + \mathbf{E_i}\ , \tag{12}$$

Writing Eq. (12) in an explicit way for $\mathbf{x}_i$,

$$\mathbf{x_i} = \left[\left(\mathbf{A_i} - \mathbf{C_i}.\mathbf{P_{i-1}}\right)^{-1}.\mathbf{B_i}\right].\mathbf{x_{i+1}} + \left(\mathbf{A_i} - \mathbf{C_i}.\mathbf{P_{i-1}}\right)^{-1}\left(\mathbf{C_i}.\mathbf{q_{i-1}} + \mathbf{E_i}\right) \tag{13}$$

For consistency of the formulas, Eqs. (13) and (9) are then compared, leading to the following recursive expressions:

$$\mathbf{P_i} = \left[\left(\mathbf{A_i} - \mathbf{C_i}.\mathbf{P_{i-1}}\right)^{-1}.\mathbf{B_i}\right] \tag{14}$$

and

$$\mathbf{q_i} = \left(\mathbf{A_i} - \mathbf{C_i}.\mathbf{P_{i-1}}\right)^{-1}\left(\mathbf{C_i}.\mathbf{q_{i-1}} + \mathbf{E_i}\right) \tag{15}$$

Once those matricial coefficients are calculated, the back substitution provides quite mechanically all elements of vector x_i. The use of this algorithm makes the systems of equations to be more diagonally dominant and the diagonal dominance is improved by the fact that the $\boldsymbol{A}_i$ coefficients are increased at the same time the $\boldsymbol{E}_i$ source terms are decreased.

3. SIMULATION PROCEDURE

For the simulation, the roof has been represented by 5 layers: mortar (1 cm), brick (10 cm), mortar (1cm), sealing layer and sand (3 cm), as shown in Fig. (1).

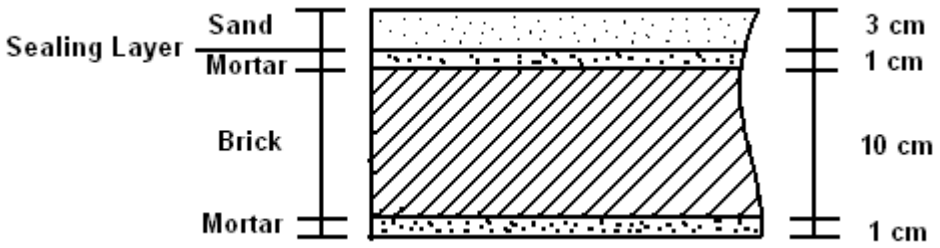

Figure 1: Physical domain of the roof.

The differential equations of energy and mass conservation for each node of the roof were discretized by using the finite-volume method (Patankar, 1980), with a central difference scheme, a uniform grid and a fully-implicit approach. The solution of the set of algebraic equations was obtained by using the MTDMA (Multi-TriDiagonal-Matrix Algorithm - Mendes et al., 2002). In the roof model, a regular mesh of 2 mm was utilized for each control volume.

In this work, the highly temperature and moisture dependent sand properties were gathered from Oliveira *et al.* (1993) and the mortar and brick properties were obtained from Perrin (1985). Their dry-basis properties are shown in Tab. (1)

Table 1: Dry-basis properties of the materials.

Material	ρ_0 (m³/kg)	c_m (J/kg K)	porosity
Sand	1650	800	0.38
Mortar	2050	932	0.18
Brick	1900	920	0.29

Figures 2 and 3 show the values of temperature, relative humidity and total solar radiation in January 31st from Test Reference Year (TRY) weather data for the city of Curitiba-Brazil.

The internal region of the roof (Fig. 1) was considered with constant values of temperature and relative humidity of 24°C and 50 % with a constant convection heat transfer coefficient of 3 W/m²K, representing, in this way, a conditioned building space. The external region were submitted to the TRY (Test Reference Year) weather data for the city of Curitiba-Brazil (South latitude of -25.2°), with a constant convective heat transfer coefficient of 12 W/m²K and a solar absorptivity of 0.5 for both sand and mortar.

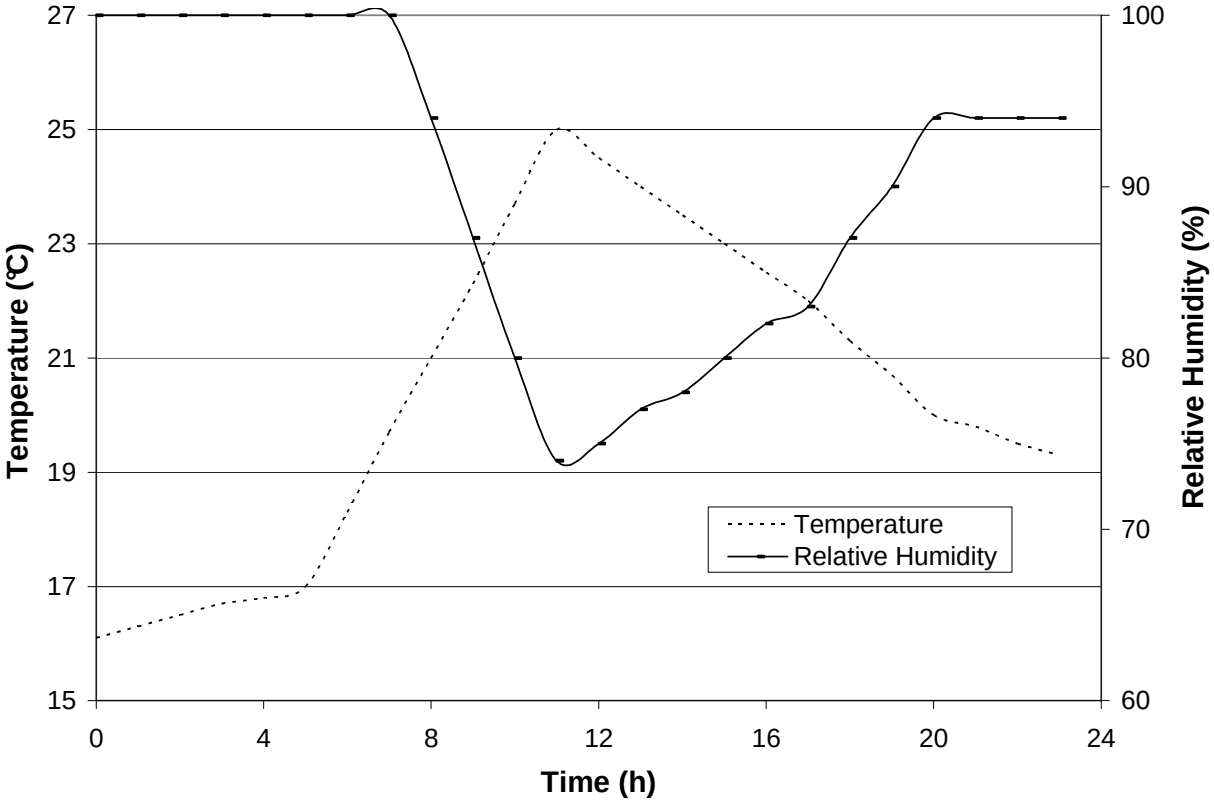

Figure 2: Values of temperature and relative humidity for Curitiba – Brazil, on January 31st .

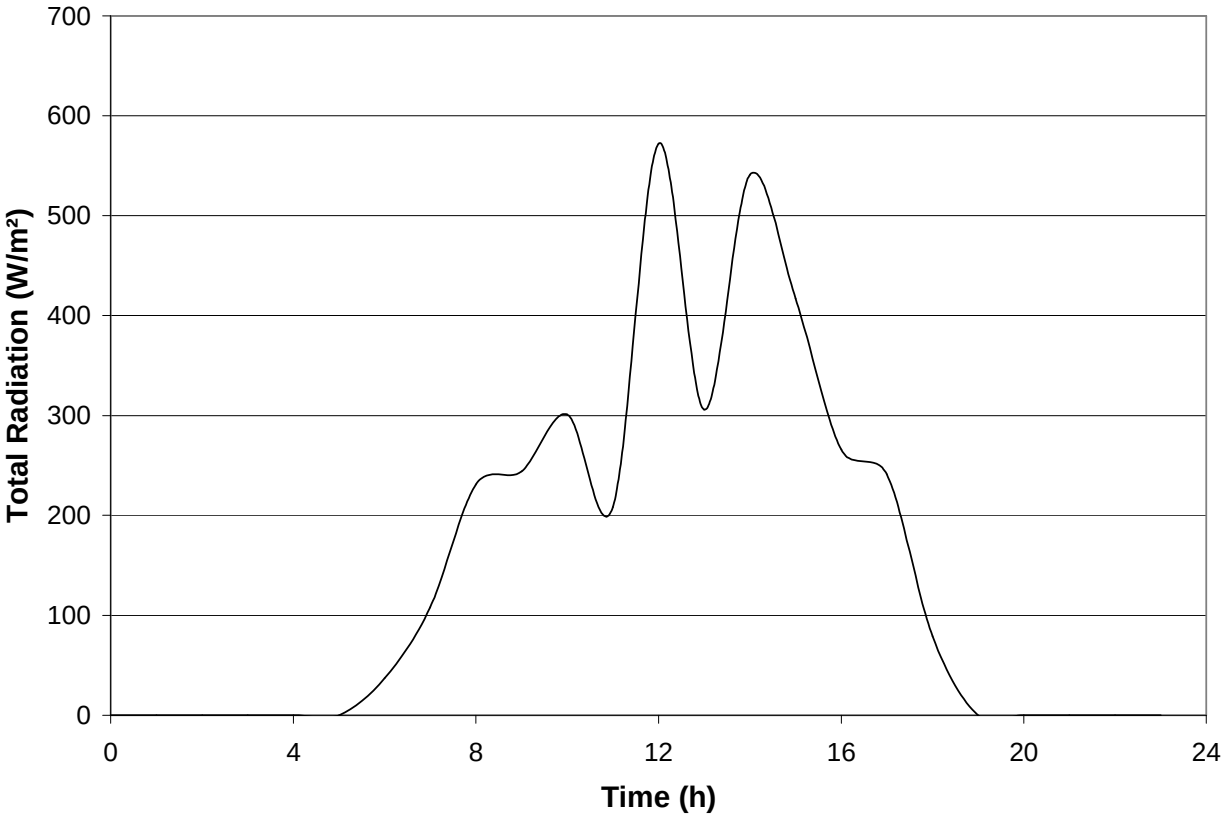

Figure 3: Values of total solar radiation for Curitiba – Brazil, on January 31st.

4. RESULTS

In order to predict the sand layer effect on building passive cooling, the Curitiba-Brasil TRY weather data file has been chosen and simulations have been carried out from Jan. 1st to Jan. 31st, using a 30-sec simulation time step. The results presented in Figs. (4) and (5) were obtained for January 31st for reducing the initial conditions effects.

Simulations in the roof were performed with or without a sand layer. It can be noticed in Fig. (4), temperature differences close to 2°C for peak values. The cooling effect was observed during daylight period, between 10 am and 6 pm, with different behavior in the night period. As observed in Fig. (5), the small difference on the external surface temperature (with or without sand layer) shows that the sand layer inertia effect is dominant when compared to the one from evaporative cooling.

Figure (5) also shows that evaporation at the external surface during the daylight period is counterbalanced by solar radiation. On the other hand, in Fig. (4), a lower relative humidity at the internal surface is observed for the roof composed by the sand layer, which contributes for indoor thermal comfort due the increment on the vapor exchanged between the air and the internal surfaces.

An interesting physical aspect noticed in Fig. (5) is the relative humidity at the sand surface. As the external surface temperature decreases below the dew point due to the negative net radiation balance at the surface, the sand becomes saturated at the surface for a 9-h period and then dries out rapidly thanks to the high short-wave radiation on the horizontal surface during day time. As the Luikov number is low and the sand is very thermal capacitive, this effect does not have much influence on the temperature.

Those differences shown in Figs. (4) and (5) could have been higher under the presence of a warmer and dryer climate and for floating indoor temperature and moisture content.

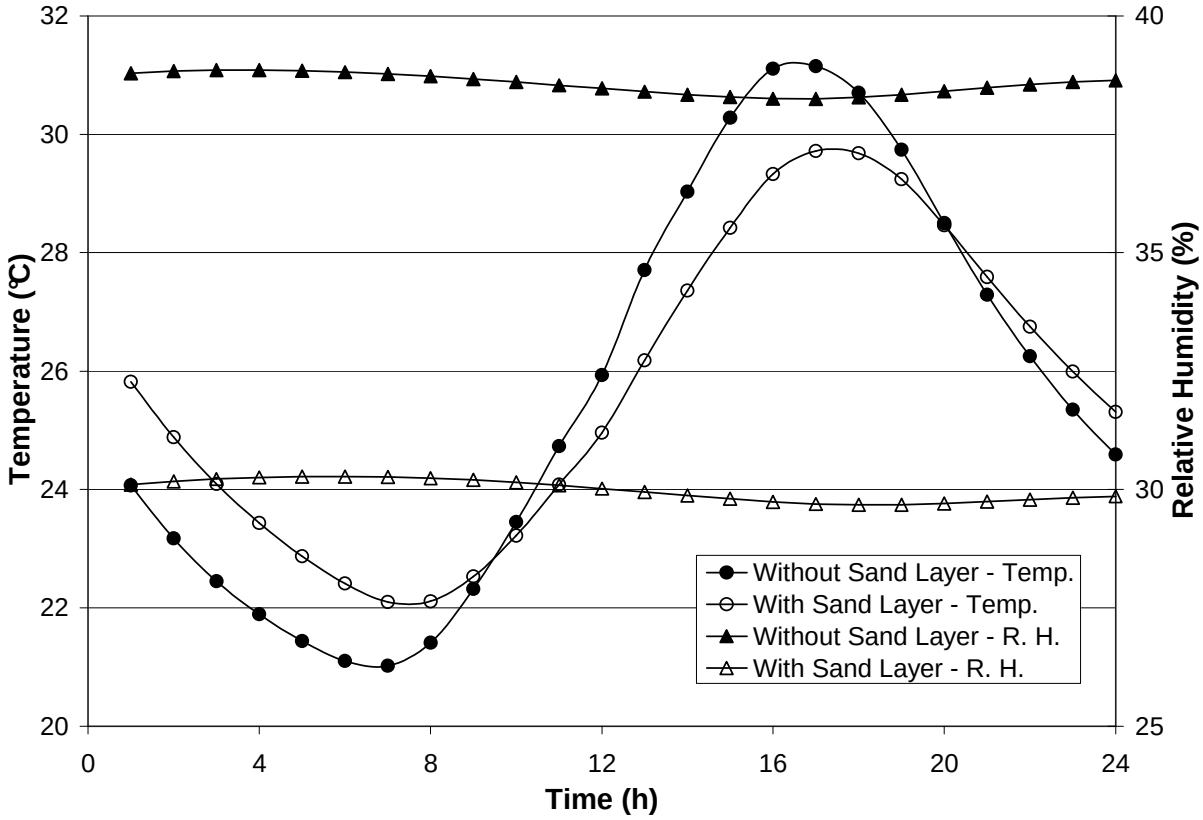

Figure 4: Temperature and relative humidity at the internal surface of the roof on January 31st.

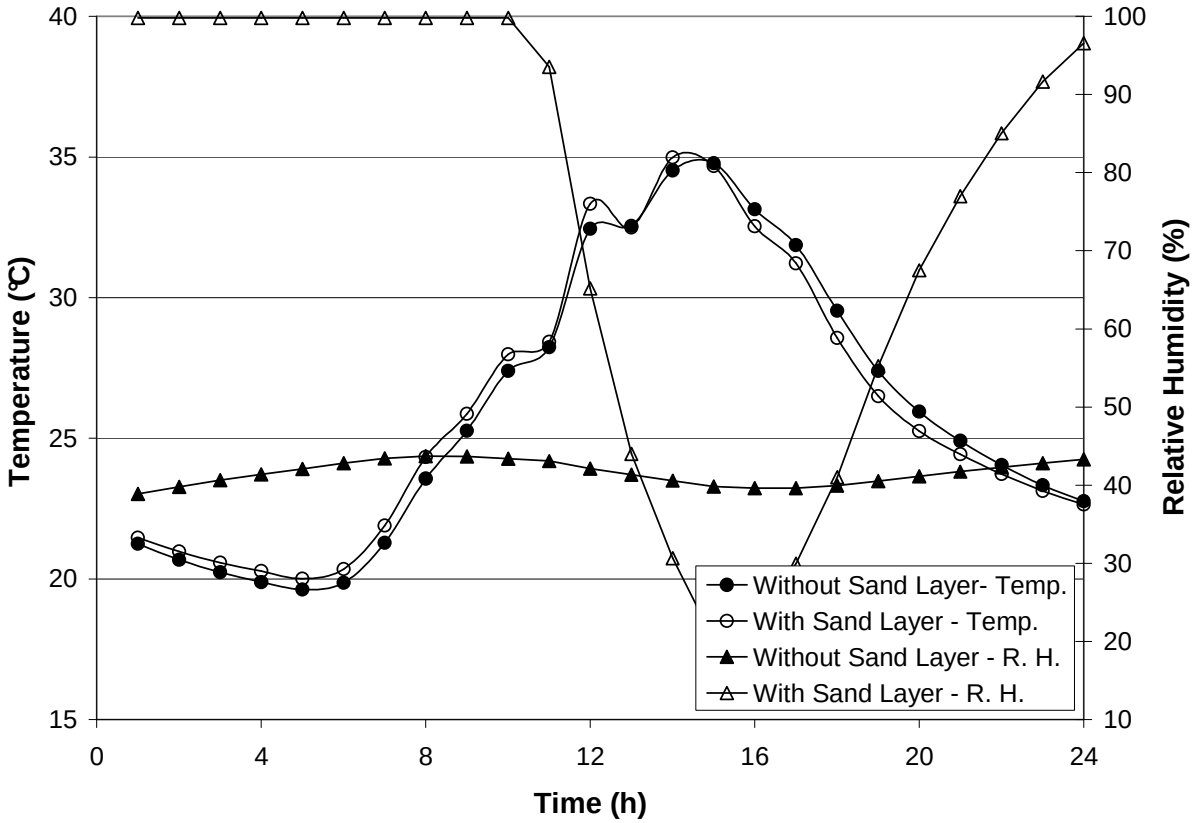

Figure 5: Temperature and relative humidity at the external surface of the roof on January 31st.

5. FINAL REMARKS

A mathematical model to simulate an unsaturated highly capacitive porous material on roof has been presented in order to predict thermal and hygric effects on building passive cooling. The weather data of Curitiba-Brazil has been used to represent external boundary conditions and comparisons in terms of temperature and relative humidity at the roof surfaces were presented.

The cooling effect was observed in the daylight period, between 10 am and 6 pm, differently from the behaviour at night time. The results showed that the inertial effect of the sand layer is higher than the evaporative cooling effect, especially due to the short-wave radiation during day time that counterbalances the latent heat flux. On the other hand, it has been observed that a lower relative humidity, at the internal roof surface composed by sand layer, can contribute for improving indoor thermal comfort. More significant differences could have been presented under the presence of a warmer and drier weather data or indoor variable conditions. In the near, a lumped transient approach for the room air domain will be considered and different climates and thickness of the sand layer will be analyzed.

6. REFERENCES

Liu, W., Peng, S. W., Mizuk, K., 1997, “Moisture Evaporation and Migration in Thin Porous Packed Bed Influenced by Ambient and Operating Conditions”, International Journal of Energy Research, V. 21, pp. 41-53.

Mendes, N., Philippi, P. C., Lamberts, R., 2002, “A new mathematical method to solve highly coupled equations of heat and mass transfer in porous media” International Journal of Heat and Mass Transfer, Vol. 45, pp. 509-518.

Meng, Q, Hu, W., 2005, “Roof cooling effect with humid porous médium”. Energy and Buildings, V. 37, pp. 1–9.

Oliveira, A. A. J; Freitas, D. S., 1993, “Influência do Meio nas Difusividades do Modelo de Phillip e Vries.”, Relatório de Pesquisa, UFSC, 1993.

Patankar, S.V., 1980, “Numerical Heat Transfer and Fluid Flow”, Hemisphere Publishing Corporation.

Perrin, B., 1985, “Etude des Transferts Couplés de Chaleur et de Masse dans des Matériaux Poreux Consolidés non Saturés Utilisés en Génie Civil", Thèse Docteur d'Etat, Université Paul Sabatier de Toulouse, Toulouse, France.

Philip, J. R., de Vries, D. A., 1957, “Moisture movement in porous media under temperature gradients” Trans. Am. Geophysical Union, Vol. 38, pp. 222-232.

Santos, G. H., Mendes, N., 2009, “Combined Heat, Air and Moisture (HAM) Transfer Model for Porous Building Materials”, Journal of Building Physics, V. 32, pp. 203-220.

Santos, G. H., Mendes, N., 2009, “Heat, Air and Moisture Transfer Through Hollow Porous Blocks, International Journal of Heat and Mass Transfer, V. 52, pp. 2390-2398.

Santos, G. H., Mendes, N., Philippi, P. C., 2009, “A Building Corner Model for Hygrothermal Performance and Mould Growth Risk Analyses, International Journal of Heat and Mass Transfer, V. 52, pp. 4862-4872.

Wang, J., Hagentoft, C. E., 2001, “A Numerical Method for Calculating Combined Heat, Air and Moisture Transport in Building Envelope Components”, Nordic Journal of Building Physics, V. 2.

7. RESPONSIBILITY NOTICE

The authors are the only responsible for the printed material included in this paper.